Gas-Phase Polymerization of Propylene with a Highly Active Ziegler-Natta Catalyst

Job Jan C. Samson, Bart van Middelkoop, Günter Weickert, and K. Roel Westerterp
Industrial Polymerization Processes, Dept. of Chemical Engineering, Twente University of Technology,
7500 AE Enschede, The Netherlands

The polymerization of propylene in the gas phase has been studied with the same high-activity catalyst as was used for liquid-phase polymerizations in earlier work. Catalyst injection, the influence of the support bed, and precontacting of the catalyst with the cocatalyst and the electron donor have been investigated. Furthermore, different ways of prepolymerization were tested. The kinetics can be described with the same model as was used for the liquid-phase polymerizations. The reaction rate was proportional to the pressure at pressures above 5 bar; at lower pressures the rates are lower. Comparison of the reaction rates in the gas phase and liquid phase showed the rates in the gas phase were still lower than in the liquid phase. The fast decay observed in the gas-phase polymerizations indicated that thermal runaway and deactivation may occur at temperatures above 40−45°C.

Introduction

Since the mid-1980s, there has been a shift in the industry from slurry and liquid to gas-phase polymerizations of olefins. Today, gas-phase polymerization may even be the most important olefin polymerization process due to its relative simplicity and flexibility. Moreover, gas-phase polymerizations offer a wide range of products, including low molecular-weight polymers.

In the public literature about olefin polymerizations with highly active catalysts there is a lack of kinetic data that can be used for reactor design and control of polymer properties. A reason for this could be that olefin polymerizations on a small scale are rather difficult to execute, and translating the results to large-scale industrial processes is also hard, because of the many pitfalls encountered. In this article we investigate the gas-phase kinetics of a highly active $MgCl_2$/$TiCl_4$ catalyst, with ethylbenzoate (EB) as the internal and paraethoxyethylbenzoate (PEEB) as the external electron donor. The catalyst has been used in conjunction with triethylaluminum (TEAl) as cocatalyst. The experiments were executed in a glass reactor at pressures up to 10 bar, and the results are compared with those obtained in the liquid phase in our earlier work (Samson et al., 1998).

Experimental Setup

The experimental setup is shown in Figure 1. It comprises a jacketed, glass reactor of *Büchi* of one liter for pressures up to 12 bar; an evaporation unit; purification units for propylene, pentane, nitrogen, and hydrogen; an injection system for small amounts of catalyst; and a temperature-control system. Propylene and pentane are purchased at a high purity and are further purified in the liquid phase in successive beds of BASF R3-11 catalyst and molecular sieves of the types 3A, 4A and 13X; hydrogen and nitrogen are purified in the same way, but in the gas phase. For a detailed description of the purification units, the temperature-control system, and material handling, the reader is referred to the article describing the liquid-phase polymerizations (Samson et al., 1998).

The purified liquid propylene is stored and fed via a dosage vessel into an 8-L evaporator. Propylene gas from the evaporator is fed into the reactor via a mass-flow controller. To prevent condensation of propylene, the lines from the evaporator to the mass-flow controller and the reactor are heated up to 60°C. Reactor pressure and temperature are measured using an electronic pressure gauge and thermocouples, respectively. The reaction is executed at a constant temperature and pressure; the reaction rate as a function of time is

---

Correspondence concerning this article should be addressed to G. Weickert.

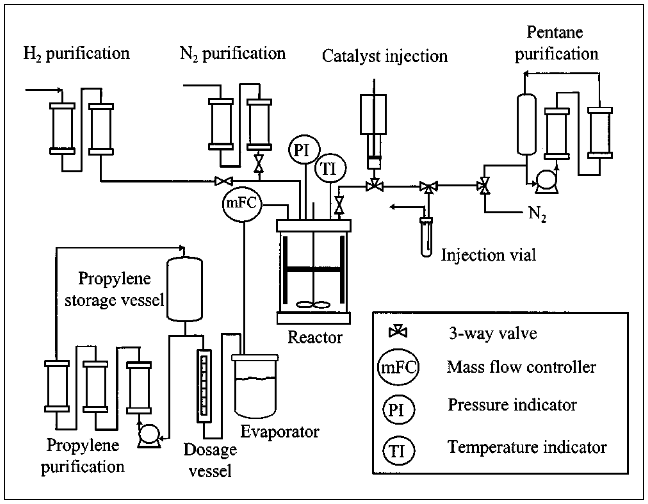

Figure 1. Experimental setup for the gas-phase polymerizations.

calculated from the feed rate required to keep the reactor pressure constant.

Mixing

Good mixing of the polymerizing particles and the surrounding gas is essential for reaction heat removal and to prevent thermal runaway in the particles, which would result in low yields and poor polymer quality. In the present work a glass reactor was used, which enables the operator to visually observe the mixing state. Figure 2 shows that the agitator used consists of two stirrers mounted on the same shaft. The upper stirrer consists of four vertical blades. To prevent powder sticking to the wall and to improve the heat transfer to the reactor jacket, two blades have a clearance of one millimeter from the reactor wall, while the other two blades are placed closer to the stirrer shaft to also provide mixing in the center. To further improve the mixing, the horizontal bars supporting the blades are shaped like propellers. The lower stirrer is a propeller that has been mounted to stir up the powder on the bottom end of the stirrer shaft, 1 mm above the reactor bottom. Because the agitator is rather heavy and rotating at 1 mm from the glass wall with rotation speeds up to 1,500 rpm, an additional bearing had to be constructed to balance the stirrer and to prevent it from touching the reactor wall.

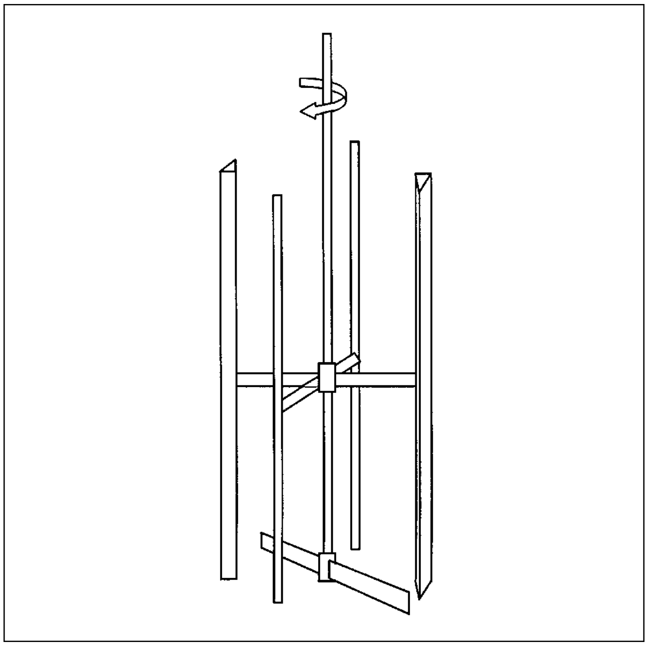

Figure 2. Agitator for the gas-phase polymerizations.

Support bed

We used a certain number of inert particles as a support bed to prevent the catalyst particles from sticking to each other and to the reactor walls. Without a support bed, the injected catalyst easily gets stuck on the reactor walls, which results in bad reproducibility and low activity. Initially, polypropylene powder was tested as a support bed: the yields obtained were far too low. Probably, the impurities in the porous polypropylene particles of the support bed are too numerous and too difficult to scavenge in the cleaning procedure. A further problem is the separation of the polypropylene support bed and the polymer produced. Therefore, we used a support bed of dried NaCl crystals. These crystals are nonporous, can be easily dried in a vacuum oven at temperatures above 100°C, and enable us to mix the catalyst properly throughout the reactor while preserving its activity. Furthermore, at the end of the reaction the polymer powder produced can be separated from the support bed by washing with water.

Catalyst injection

To inject the catalyst, the same method was used as in the liquid-phase experiments; see Figure 3. The catalyst compo-

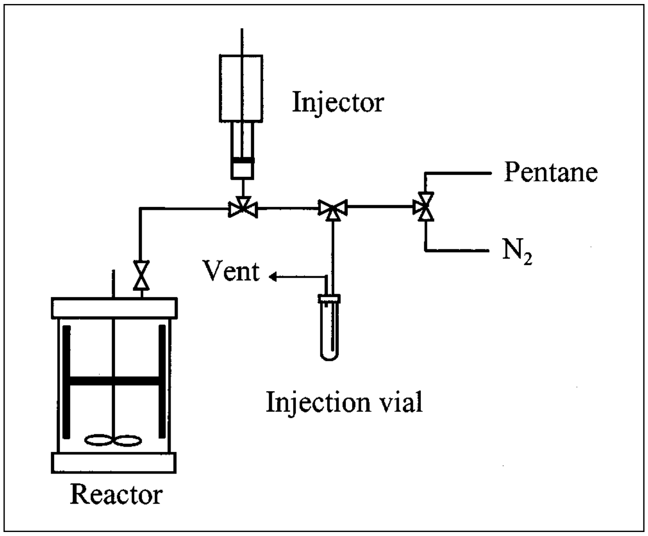

Figure 3. Catalyst injection system.

nents were prepared and weighted in a 20-mL vial in an inert atmosphere. After the vial was sealed with a rubber septum, it was connected to the reactor by two sharpened capillaries, which were continuously flushed with nitrogen to avoid contamination. Then the three-way valve above the vial was then opened to add a few milliliters of pentane through one of the capillaries to the vial. After that, the catalyst was suspended in the pentane and the contents were sucked into the injector by the continuous shaking action of the vial. The contents were then injected into the reactor. The injection procedure was repeated several times with fresh pentane to flush the vial and lines to the reactor and to avoid catalyst losses.

The injection method just described is effective for highly active catalysts because suspension of the catalyst in an inert hydrocarbon enhances deagglomeration, minimizes the effective size of the catalyst particles, and helps to avoid the thermal runaway of particles. One drawback of using this injecting method is the introduction of liquid. Although the amount of liquid introduced into the reactor is relatively small (10 to 15 mL), it has to be removed from the reactor to have pure, gas-phase monomer around the particles. Leaving the liquid in the reactor results in a concentrated slurry reaction rather than a gas-phase reaction, at least in the first stage of the reaction. Later on, the liquid may be completely absorbed in the formed polymer, but even then it will influence the propylene concentration in the polymer. It is therefore essential that the liquid be removed from the reactor. We have used the relatively volatile pentane as liquid and removed it by evaporation through repeated pressurization and venting with propylene. Depending on the reactor temperature, two to five cycles of pressurization to 10 bars and subsequent venting to atmospheric pressure proved to be more than sufficient to evaporate all the liquid from the reactor. Evaporation can be completed within 5 min, as one pressurizing and venting cycle takes about one minute. The possible losses of cocatalyst and electron donor by entrainment with the evaporating liquid are assumed to be negligible, because the boiling points of these components are above 200°C.

Precontacting

The catalyst performance is strongly influenced by the sequence in which the catalyst, cocatalyst, and electron donor are contacted. Contrary to the liquid-phase experiments, where the cocatalyst, electron donor, and catalyst were injected sequentially in that order at one-minute intervals, we precontacted the catalyst with the electron donor and/or cocatalyst prior to injection. This reduces the amount of liquid injected into the reactor.

Two methods of precontacting were applied. First, the catalyst was precontacted with only PEEB before being injected into the reactor with pentane. In this case, the catalyst/PEEB slurry was injected after the cocatalyst. Precontacting of the catalyst with PEEB resulted in a temporary poisoning of the active sites with PEEB for about 5 min. The pentane can be removed from the reactor during this period.

Second, the catalyst was precontacted with the cocatalyst *and* electron-donor mixture prior to injection. In this case, the reaction started immediately after the catalyst/PEEB/TEAl slurry was injected into the reactor.

Polymerization Procedures

Polymerization procedure

Before each experiment the reactor was thoroughly cleaned with refined petrol, and then dried. A support bed of 20 g of dried NaCl was then added to the reactor and the reactor was closed and flushed with nitrogen. After evacuating the reactor at 75°C for 3 h, it was kept under nitrogen pressure overnight. The next day the reactor was evacuated for 45 min at 75°C, followed by repeated pressurization and venting with propylene. Under intensive stirring, 200 mg of TEAl was injected into the reactor with about 40 mL of pentane, to remove the remaining impurities from the reactor. After 30 min the pentane was removed from the reactor in three to five cycles of pressurization and venting with propylene, each cycle taking about one minute. After the clean reactor was heated to the desired reaction temperature, the catalyst components were injected. In the case where the catalyst was precontacted with only electron donor, the cocatalyst was first injected with pentane. After removal of the pentane from the reactor, the catalyst/PEEB slurry was injected, followed by removal of the pentane. In the case where the catalyst was precontacted with the cocatalyst *and* electron donor, all catalyst components were injected together.

After the catalyst injection and the evaporation of pentane, a prescribed amount of hydrogen was fed to the reactor and the desired monomer pressure was set. The reaction rate was obtained by measuring the mass flow of propylene to the reactor required to keep the pressure constant. After 75 min, the reaction was stopped by neutralizing the catalyst with a few milliliters of methanol. The polymer product was washed with water to separate the NaCl support bed and dried in a vacuum oven at 50°C overnight: a dry, free-flowing powder was obtained.

Prepolymerization

Prepolymerization is a precisely controlled polymerization under mild reaction conditions that precedes the polymerization process itself. It is intended to prevent a thermal runaway of the particles and their disintegration into fines, by controlling the heat production and the fragmentation of the catalyst, respectively. Several prepolymerization methods have been tested. Initially, prepolymerization was performed in the reactor itself for a few minutes at a low temperature; after that the temperature was raised as fast as possible to the desired reaction temperature. This method, used with success in liquid pool polymerizations, failed in gas-phase polymerizations because it takes 15 to 30 min to heat the glass reactor to the required temperature, so an important part of the reaction rate data was lost. Therefore, the prepolymerization had to be performed outside the reactor. Figure 4a shows the prepolymerization in the vial. After dilution of the catalyst with pentane, a mixture of propylene and nitrogen was bubbled through the catalyst suspension at ambient temperature in 10-s intervals. The propylene supply was interrupted for one minute after each 10-s interval to keep the temperature from rising. This prepolymerization method was moderately successful because of plugging of the capillaries. Therefore, a small prepolymerization bubble column, with a diameter of 2 cm and a volume of 25 mL, was developed

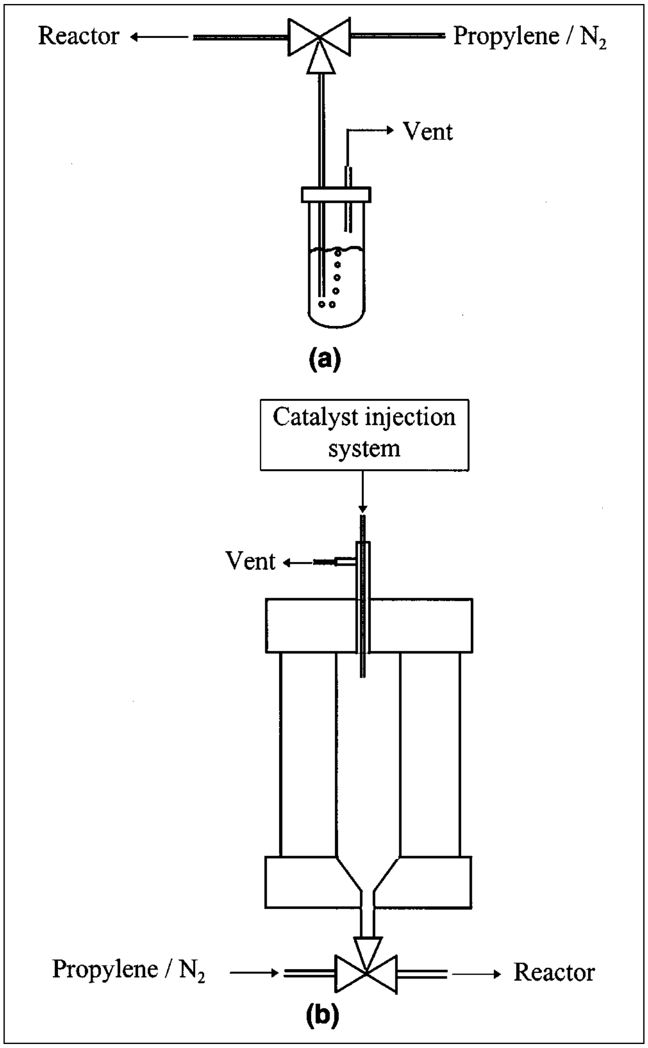

Figure 4. Prepolymerization: (a) in the vial before catalyst injection; (b) in the prepolymerization reactor.

(see Figure 4b). The catalyst components were injected into this reactor simultaneously with about 10 mL pentane. Again, to prepolymerize the catalyst, gaseous propylene was bubbled through the catalyst suspension in 10-s intervals at ambient temperature. After each 10-s interval, the propylene supply was interrupted for one minute to avoid overheating. After a period of a few minutes, the gas flow was stopped and the prepolymerized catalyst injected into the reactor via a three-way valve. The rest of the procedure is similar to the polymerization procedure described before.

Kinetics

Kinetic model

The kinetic model used to describe the gas-phase kinetics is the same as was used for the liquid-phase kinetics. The model is based on the assumptions that the polymerization rate is first order in the propylene concentration and that the deactivation rate is second order in the number of active centers (Doi et al., 1982; Samson et al., 1998). The model is briefly described below:

$$R_p = k_p C_m C^*, \tag{1}$$

with $k_p = k_{p,0}\cdot e^{(E_{a,p}/RT)}$, where k_p is the lumped propagation rate constant, and $E_{a,p}$ is the lumped activation energy for the propagation reactions. The catalyst decay is described by a decrease in the number of active centers over time, according to the following equation:

$$-\frac{dC^*}{dt} = k_d (C^*)^2, \tag{2}$$

with $k_d = k_{d,0}\cdot e^{(-E_{a,d}/RT)}$, where k_d is the lumped deactivation constant, and $E_{a,d}$ is the lumped activation energy for the different deactivation reactions. Combining Eqs. 1 and 2 gives

$$-\frac{dR_p}{dt} = K_D \cdot C_m^{-1} \cdot R_p^2, \tag{3}$$

with $K_D = (k_{d,0}/k_{p,0}^{n-1})\cdot e^{[(n-1)\cdot E_{a,p} - E_{a,d}/RT]}$.

Integration of Eq. 3 gives the reaction rate as a function of time:

$$R_p = \left(R_{p,0}^{-1} + K_D \cdot C_m^{-1} \cdot t\right)^{-1} \tag{4}$$

with $R_{p,0} = k_{p,0}\cdot e^{-(E_{a,p}/RT)}\cdot C_0^* \cdot C_m$.

Finally, the yield as a function of time is calculated from the over the time integrated reaction rate:

$$Y = \frac{C_m}{K_D}\cdot \ln\left(1 + R_{p,0}\cdot \frac{K_D}{C_m}\cdot t\right). \tag{5}$$

Sorption

The sorption behavior of the monomer in the polymer is an important aspect because it relates directly to the monomer concentration C_m required in the kinetic model Eq. 5. Since experimental data about the sorption behavior of propylene in polypropylene (PP) has not been found, C_m was estimated. To have an indication of the accuracy of the estimate, C_m was estimated with both Henry's law (Hutchinson and Ray, 1990) and the Flory-Huggins sorption isotherm.

Henry's law can be applied for the sorption of relatively light propylene in polypropylene under gas-phase conditions at relatively low pressures:

$$C_m = k_H \cdot P_m, \tag{6}$$

where k_H is the Henry constant and P_m the monomer pressure. The value of the Henry constant can be calculated from the following equation (Stern et al., 1969):

$$\log(k_H) = -2.38 + 1.08\cdot(T_c/T)^2, \tag{7}$$

Table 1. Sorption Data[*]

T (°C)	Flory-Huggins C_m (kg/m^3)	Henry's Law C_m (kg/m^3)	P_{dev} (atm)	ϕ $(-)$	x_m Mass %
22	52.8	39.3	3.2	0.102	2.18
27	42.6	34.6	3.7	0.086	1.79
32	34.3	30.7	4.4	0.072	1.45
37	28.0	27.4	5.1	0.059	1.15
42	22.7	24.6	6.0	0.048	0.91
47	18.5	22.2	6.9	0.038	0.70
52	14.9	20.1	7.9	0.030	0.54
57	12.0	18.3	9.1	0.023	0.40
62	9.4	16.7	10.4	0.018	0.31

[*] The monomer concentration in the polymer C_m calculated with the Flory-Huggins sorption isotherm and Henry's law at 5-bar pressure for different temperatures together with the calculated pressure P_{dev}, at which the errors in the concentration predicted by Henry's law are larger than 5%. Also, the ϕ-values and the calculated mass fraction of monomer in the particle, the latter based on a polymer crystallinity of 60%.

where T_c is the critical temperature, and k_H is the Henry constant expressed in mol/L·atm. The validity of Henry's law is verified by the correlation given below (Stern et al., 1969):

$$\log\left(\frac{P_{\text{dev}}}{P_c}\right) = 3.025 - 3.50 \cdot \left(\frac{T_c}{T}\right) \tag{8}$$

where P_c is the critical pressure, and P_{dev} the pressure at which 5% deviation from Henry's law occurs; above P_{dev}, Henry's law is not reliable anymore (see Table 1). The monomer concentration was also estimated with the Flory-Huggins sorption isotherm:

$$\ln\frac{P}{P^0} = \ln\phi + (1-\phi) + \chi(1-\phi)^2, \tag{9}$$

where P and P^0 are the partial pressure and the saturation vapor pressure of the monomer, respectively; χ is the Flory-Huggins interaction parameter; and ϕ is the volume fraction of permeant sorbed in the amorphous parts of the polymer. Finally, the monomer concentration in the polymer C_m has been estimated by the following equation:

$$C_m = \phi \cdot C_L, \tag{11}$$

where C_L is the concentration of liquid monomer at a given temperature. For further details on the calculation of the Flory-Huggins interaction parameter χ and the volume fraction of monomer in the amorphous parts of the polymer ϕ, the reader is referred to our earlier work about liquid-phase polymerizations (Samson et al., 1998).

Table 1 shows the monomer concentrations calculated by both the Flory-Huggins sorption isotherm and the Henry's law with the corresponding values of P_{dev}. The values of P_{dev} indicate that Henry's law is not reliable for temperatures below 37°C, because for those temperatures, P_{dev} is smaller than the applied monomer pressure of 5 bar. At a temperature of 22°C, the concentration calculated with the Flory-Huggins sorption isotherm is 30% *higher* than that calculated with Henry's law; at 37°C the calculated values are equal; and at 62°C the Flory-Huggins sorption isotherm predicts a concentration that is 45% *lower* than that calculated by Henry's law.

Table 2. Monomer Solubility[*]

P (bar)	Flory-Huggins C_m (kg/m^3)	Henry's Law C_m (kg/m^3)
2.5	13.2	13.7
3	15.8	16.4
5	28.2	27.4
7.5	47.4	41.1
10	70.8	54.8

[*] The monomer concentration in the polymer C_m calculated with Flory-Huggins sorption isotherm and Henry's law at 37°C for different pressures.

Table 2 presents the monomer concentrations C_m calculated with both the Flory-Huggins sorption isotherm and Henry's law at a temperature of 37°C for different pressures. The calculated concentrations are of the same order.

In the remaining calculations we have chosen to use monomer concentrations based on the Flory-Huggins sorption isotherm, because it takes into account the polymer/monomer interactions as well as the interaction between the monomer molecules. For a polypropylene/propylene system, the interactions between the permeant molecules are relatively strong compared to the permeant/polymer interactions. This results in an increase in the Henry sorption coefficient, with an increasing volume fraction of monomer in the polymer.

Besides, since the Flory-Huggins sorption isotherm also has been used to estimate C_m in liquid-phase polymerizations, the gas- and liquid-phase results are described on the same basis.

In the 22 to 62°C temperature range and at a pressure of 5 bar, the mass fraction of monomer sorbed in the polymer particle has been estimated to be at most 2.2% (see Table 1). As the calculation of the reaction rate is based on the mass flow to the reactor as a function of time required to keep the pressure constant, the calculated rates include the sorbed but not reacted propylene, and are also at most 2.2% too high. Because the sorption effect is relatively small, it has been neglected in the calculations of the reaction rates as a function of time.

Results

Reproducibility

We have tested reproducibility by repeating the standard experiment (see Figure 5). This figure shows the reaction-rate curves of the same experiment at a temperature of 37°C and a pressure of 5 bar. The rate curves of experiments 1 and 2 are almost the same, while the rate curve of experiment 3 lies slightly lower. The deviation in yield is at most 12% from the average yield, which we find acceptable considering the cumbersome catalyst injection and evaporation procedure and the relatively small scale of the experiment. Furthermore, the heat transfer from the particles to the surrounding gas is relatively low compared to the heat transfer in the liquid phase. This makes the catalyst much more sensitive for a thermal runaway, especially at higher temperatures or when the mixing is poor. This can be seen in the 10 to 20% decrease in yield when the powder gets stuck to the reactor wall during the first minutes of the reaction. Probably the heat exchange between the particles in such a layer and the surrounding gas is

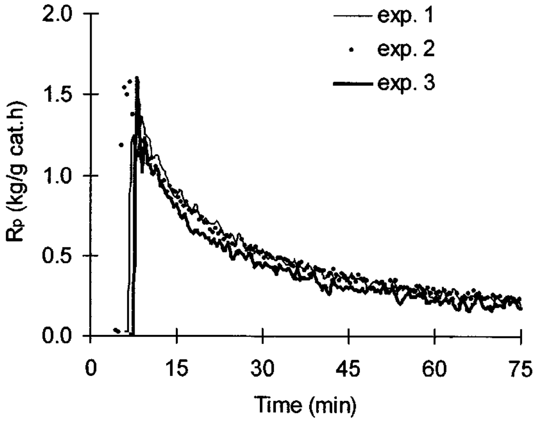

Figure 5. Reaction rate as a function of time of a repeated standard experiment at 37°C and 5 bar.

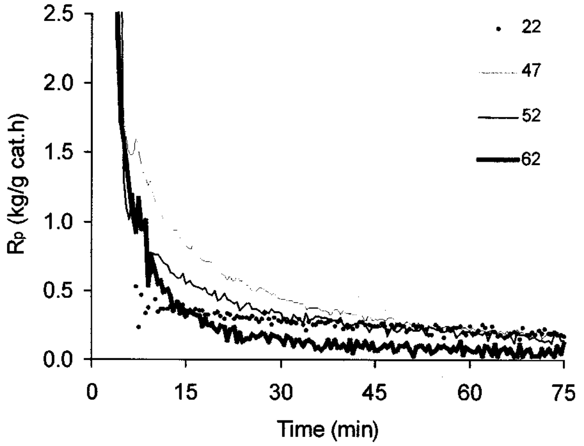

Figure 7. Typical reaction-rates at 22–62°C with a reaction time of 75 min.

too poor to avoid thermal runaway, which results in thermal deactivation.

Influence of precontacting

The influence on the reaction rates of precontacting the catalyst with PEEB alone, and the catalyst with a mixture of PEEB *and* TEAl, is shown in Figure 6. The figure shows that the highest reaction rate was obtained when the catalyst was precontacted with a mixture of PEEB and TEAl prior to injection into the reactor. In this case, the reaction starts immediately after injection, and the reaction-rate data of the first 3 to 5 min are lost because the pentane has to be removed from the reactor during this period.

When the catalyst is precontacted with PEEB only, the reaction starts about 5 min *after* catalyst injection. During the inactive period, the cocatalyst has to diffuse to the temporarily poisoned sites to form active centers. After sufficient active sites have been formed, the reaction starts; the rates are about 25% lower than when precontacting the catalyst with a mixture of PEEB and TEAl. Significant portions of the active centers are probably irreversibly poisoned by the electron donor. It is also possible that activation by the cocatalyst starts at the particle surface, immediately after which a polymer layer forms on the particle before activation of all of the potentially active sites has been completed. Due to the mass-transfer limitations in such a polymer layer, the catalyst may be incompletely activated, which results in lower polymerization rates.

Precontacting the catalyst with PEEB alone gives the operator enough time to remove the pentane from the reactor before the reaction starts. Therefore, in this case, data of the entire course of the polymerization are obtained.

Influence of the temperature

The influence of temperature on the reaction rate has been studied in a series of experiments with a 4% hydrogen concentration and a fixed ratio of catalyst, cocatalyst, and electron donor. Figure 7 shows the reaction rate curves for different temperatures. For temperatures in the 22 to 47°C range, the reaction rate increases with increasing temperature, but above 47°C, it decreases sharply. This decrease is

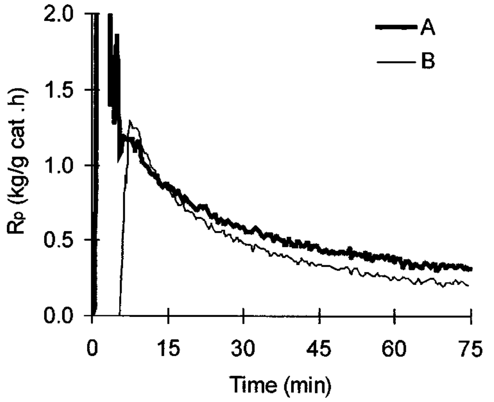

Figure 6. Average reaction rates of repeated experiments having precontacting of the catalyst with: (A) mixture of PEEB and TEAl; (B) PEEB merely.

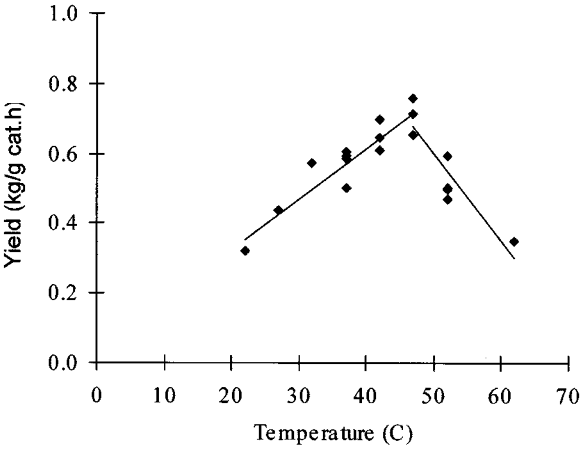

Figure 8. Polymer yield per g $MgCl_2/TiCl_4/EB$ catalyst after 75 min reaction as a function of the temperature.

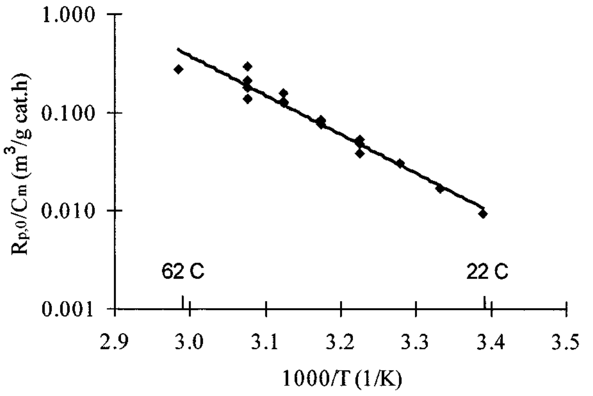

Figure 9. Arrhenius plot of the initial reaction rate ($R_{p,0}$) at 22–62°C.

also found in the yield as a function of temperature (see Figure 8). At 62°C the initial reaction rate is the highest, but the catalyst decays so fast that after 15 min the reaction rate is even lower than at 22°C.

Figure 9 shows the initial reaction rates as a function of reciprocal temperature. From the data in this figure, the activation energy of the propagation reactions has been estimated to be 76.2 kJ/mol. In Figure 10, the deactivation constant K_D is shown as a function of the reciprocal temperature: K_D decreases with increasing temperature up to 52°C, and above this temperature K_D increases. From the data in the 22 to 52°C temperature range, as given in Figure 10, the activation energy for the deactivation reactions has been estimated to be 50.6 kJ/mol. The constants for the kinetic model and the constants for the liquid-phase polymerizations are summarized in Table 3. The calculated and experimental reaction-rate curves are given for the temperatures 27 and 52°C in Figures 11a and 11b, respectively; the model describes the experiments within this temperature range moderately well.

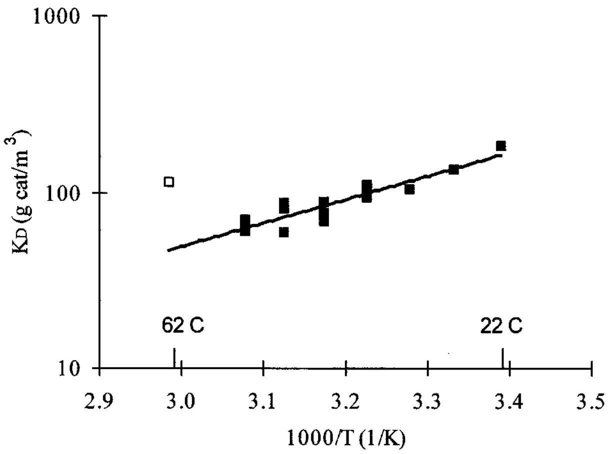

Figure 10. Arrhenius plot of the deactivation constant (K_D) at 22–62°C.

The open square □ represents the deviation constant K_D at 62°C and has not been used in the determination of the kinetic parameters.

Table 3. Constants of the Kinetic Model for Gas- and Liquid-Phase Polymerization

	Gas Phase	Liquid Phase
$E_{a,p}$ (kJ/mol)	76.2	79.9
$E_{a,d}$ (kJ/mol)	50.6	35.7
$k_{p,0} \cdot C_0^*$ (m³/g cat)	3.29×10^{11}	2.4×10^{12}
$k_d/k_{p,0}$ (m³·g cat/h)	4.8×10^{-3}	1.7×10^{-6}
Validity range (°C)	22–52	27–67

Influence of pressure

The influence of the pressure has been studied in a series of experiments at a temperature of 37°C. Figure 12 shows that the yield increases almost linearly as a function of the pressure. In Figure 13 $R_{p,0}/C_m$ is given as a function of the pressure, showing that $R_{p,0}/C_m$ is constant for pressures of 5 bar and higher, which indicates that the reaction in this pres-

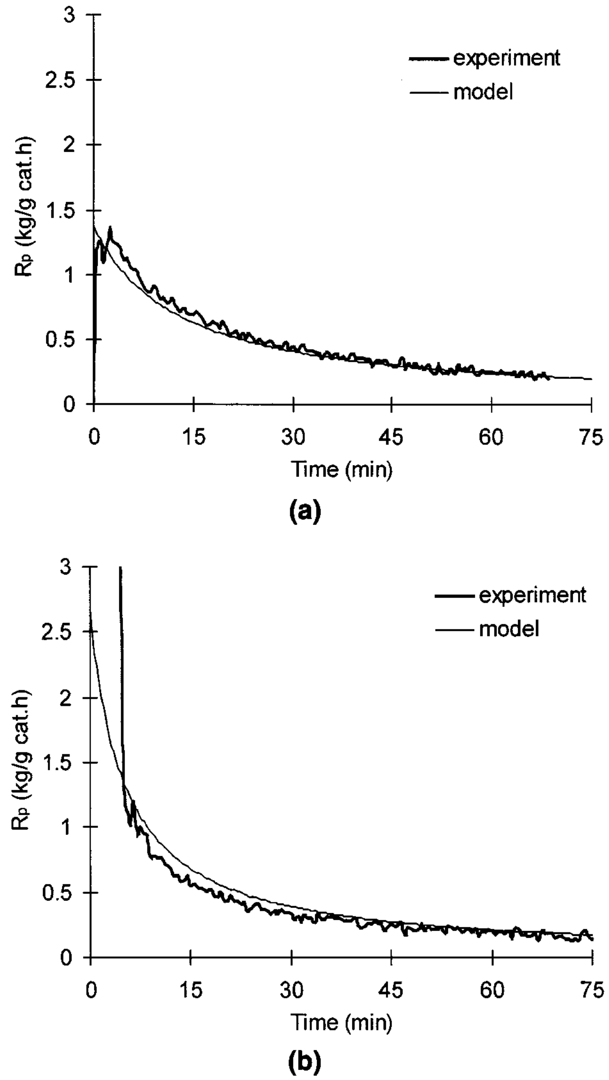

Figure 11. Experimental and simulated reaction rates of an experiment: (a) at 27°C; (b) at 52°C.

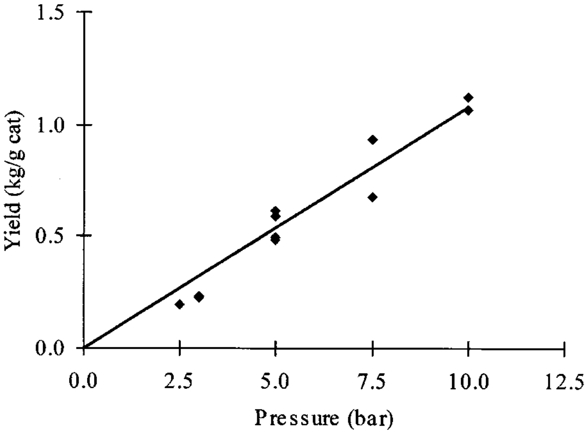

Figure 12. Yield per g $MgCl_2/TiCl_4/EB$ catalyst as function of the pressure at 37°C and after a reaction time of 75 min.

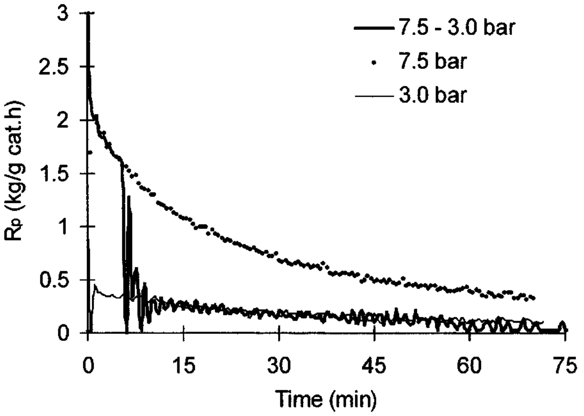

Figure 14. Reaction rates of an experiment started at 7.5 bar and decreased to 3.0 bar after 6 min, with reaction rates at 3.0 and 7.5 bar.

sure range is first order in the monomer concentration. For pressures below 3 bar, $R_{p,0}/C_m$ is considerably lower. The reason for this deviation from first-order kinetics in the monomer concentration at lower monomer pressures is not clear. The reaction rate may be of an order below one in the monomer concentration, or a part of the sites may not be active at lower pressures. Figure 14 shows the reaction-rate curve of an experiment that was performed at a pressure of 7.5 bar for 6 min, and for the remaining reaction time at 3.0 bar, together with the reaction-rate curves measured at 3.0 and 7.5 bar. In the first period, the reaction follows exactly the course of the rate at 7.5 bar, and after that exactly the course as measured for the experiment at 3.0 bar. This confirms that the low rate at the lower pressures is determined by the intrinsic kinetics.

Influence of prepolymerization

The influence of prepolymerization in pentane at ambient temperature was tested for a reaction at a temperature of 47°C (see Figure 15). This figure shows the reaction-rate curves obtained with and without prepolymerization; in both cases the catalyst, cocatalyst, and electron donor have been precontacted. Prepolymerization increases the reaction rate, especially during the first 30 to 45 min of the reaction; the yield increases by about 15%. Prepolymerization followed by reaction at 52°C has given similar results. The increase in activity as a result of prepolymerization is of the same order as that obtained with prepolymerization in liquid-phase experiments.

Comparison of gas- and liquid-phase experiments

The results of the gas-phase experiments are compared to the liquid-phase results obtained earlier (see Samson et al., 1998). This comparison is of interest because the experiments were performed with the same batches of catalyst components and of propylene. Our hypothesis is that the same catalyst activity may be expected in the gas and liquid phases if the ratios between catalyst, cocatalyst, and electron donor are

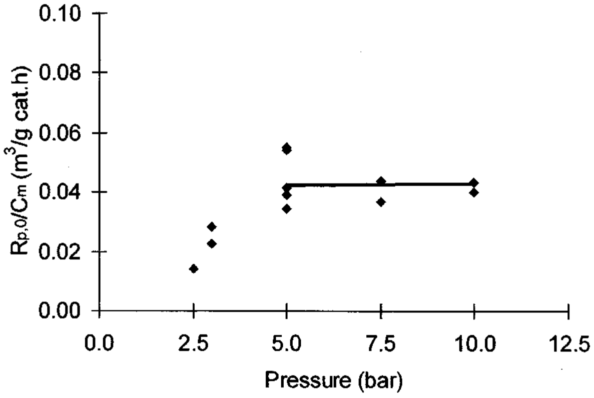

Figure 13. $R_{p,0}/C_m$ as a function of the pressure at 37°C.

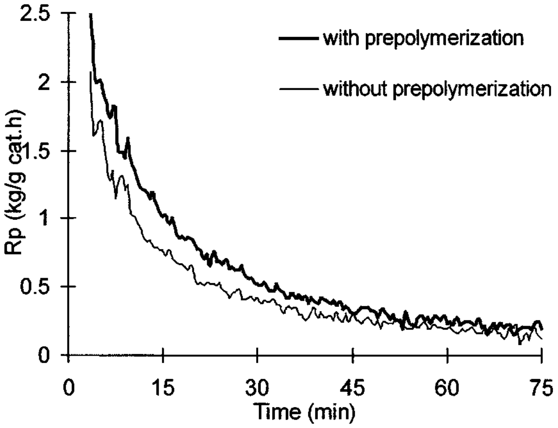

Figure 15. Influence of 3-min prepolymerization at ambient temperature on the reaction rate for an experiment at 47°C.

the same. In this case, both phases consist of pure monomer and the reaction mechanism is identical. The major differences between reactions in the gas and liquid phases are the concentration of the monomer, the value of the heat-transfer coefficient from the particle to the bulk phase, and the mobility of the cocatalyst and electron donor. In order to make an accurate comparison of the catalyst activity, the reaction rates were divided by the monomer concentration in the polymer. The ratio of the liquid- and gas-phase reaction rates, divided by the monomer concentration in the polymer, is given by

$$r_{L/G} = \frac{\left(\dfrac{R_p}{C_m}\right)_L}{\left(\dfrac{R_p}{C_m}\right)_g}. \tag{12}$$

When the number of active centers is assumed to be equal in gas- and liquid-phase polymerizations, the reaction rates in the liquid and gas phases are the same when $r_{L/G} = 1$ (see Eq. 1). Figure 16 shows that the Arrhenius plots of the liquid and gas phases have the same slope, whereas the initial reaction rates are about 40% lower in the gas phase. The agreement between the results can still be described as moderately good, considering the large differences between the experiments: the precontacting of the catalyst with PEEB, which has been applied in the gas phase, reduces the catalyst activity by about 25%, and the large differences in C_m itself and the uncertainty of the estimates of C_m. Furthermore, the experiments have proved to be very sensitive to small errors. The constants of the kinetic model described earlier (see Eqs. 1–4), are given in Table 3 for both the gas- and liquid-phase reactions. To give an idea of the results, Table 4 shows the calculated values of $R_{p,0}/C_m$ and K_D for temperatures of 30 and 50°C. In the gas phase, $R_{p,0}$ is about 40% lower than in the liquid phase for both temperatures, whereas the ratio of the K_D values in the gas and liquid phases increases with increasing temperature, so the deactivation rate in the gas phase increases more rapidly with increasing temperatures.

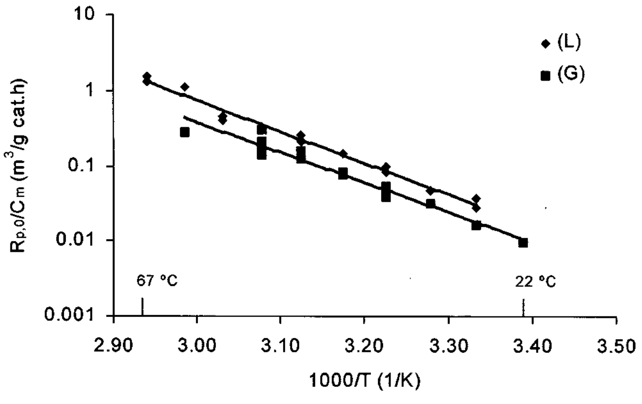

Figure 16. Initial reaction rates $R_{p,0}/C_m$ of the gas- and liquid-phase experiments as a function of the reciprocal temperature.

Table 4. Calculated Results of Kinetic Parameters in the Gas and Liquid Phase at 30 and 50°C

Parameter	Calc. Values Gas-Phase Kinetics	Calc. Values Liquid-Phase Kinetics
$R_{p,0}/C_m$ (at 30°C)	0.024 (m^3/g cat·h)	0.04 (m^3/g cat·h)
K_D (at 30°C)	124.3 (g cat/m^3)	70.9 (g cat/m^3)
$R_{p,0}/C_m$ (at 50°C)	0.16 (m^3/g cat·h)	0.28 (m^3/g cat·h)
K_D (at 50°C)	66.2 (g cat/m^3)	18.4 (g cat/m^3)

Figures 17a to 17e gives R_p/C_m as a function of time. Each part of the figure shows the rate curves—that is, R_pC_m vs. time—of the gas- and liquid-phase experiments for the same temperature. Each curve is composed of the averages of the reaction rates of repeated experiments. Notice that the reaction-rate curves obtained in the gas phase have been multiplied with $r_{L/G}$ to compare the course of the reaction in the gas and liquid phases. Remarkably, the curves of the gas- and liquid-phase experiments are almost identically shaped in the lower temperature range. For temperatures above 47°C the gas-phase curves lie above those of the liquid phase during the first 5 to 15 min. In the gas-phase experiments, the catalyst decays significantly faster during this first period; after that the rate follows the same course as in the liquid phase. This rapid decay in the gas phase becomes more pronounced as temperatures increase, and is probably the result of a thermal runaway of the particles.

Figure 18 shows the ratio of the liquid and gas reaction rates, $r_{L/G}$, as a function of the temperature. For temperatures from 22°C to 37°C, the reaction rates in the gas phase are about 35% lower than in the liquid phase. Above 37°C, $r_{L/G}$ increases sharply with increasing temperature, up to a value of about 6 at 62°C. The differences and errors in the experimental procedures and estimates were of the same order for all experiments. The increase in $r_{L/G}$ with increasing temperature is therefore believed to be caused by a thermal deactivation in the gas-phase reactions. This has not been confirmed by gas-phase experiments that have a prepolymerization step. At a reaction temperature of 47°C, a prepolymerization at ambient temperature increased the reaction rates only about 15%, while $r_{L/G}$ is 2.8. It is possible the prepolymerization step was too short to prevent runaway. Prolonging the prepolymerization time resulted in flocculation of the catalyst and plugging of the pipes. To find the cause of the observed differences in the gas- and liquid-phase polymerization reaction rates, a detailed study of the polymerization has to be made. The prepolymerization temperature period and the concentrations of electron donor and cocatalyst during prepolymerization are important variables in prepolymerization. These variables determine whether the prepolymerization successfully controls the heat transfer and fragmentation process in the first stage of the reaction, while preserving the activity of the catalyst. Such a study will be part of one future investigations.

Conclusions

An experimental setup for gas-phase polymerizations with highly active catalyst systems has been described, and the re-

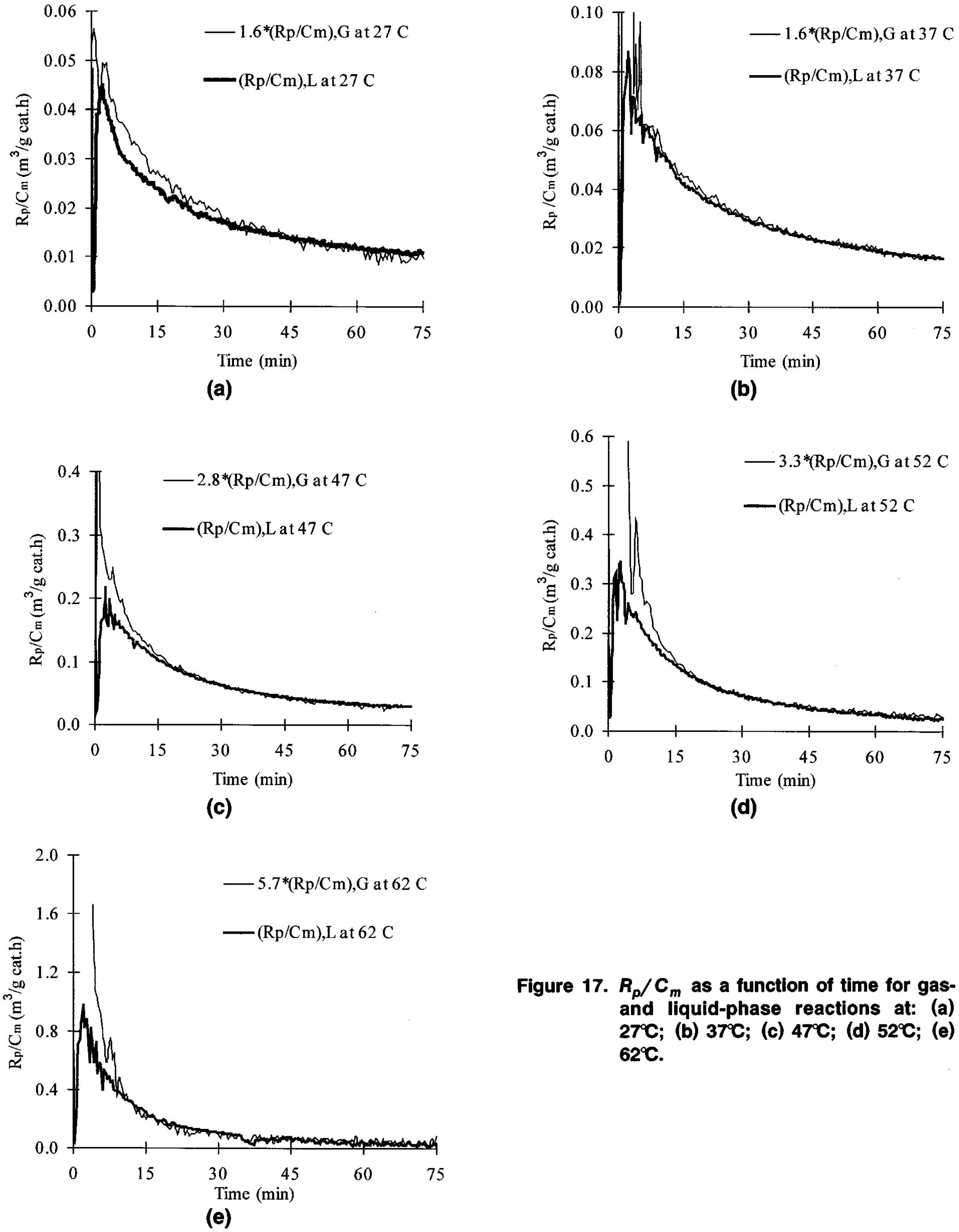

Figure 17. R_p/C_m **as a function of time for gas- and liquid-phase reactions at: (a) 27°C; (b) 37°C; (c) 47°C; (d) 52°C; (e) 62°C.**

producibility of the experiments has been tested to be within 12%. Small deviations in the polymerization procedure or mixing conditions do influence the catalyst activity and decay behavior. The experimental results show that the catalyst injection, precontacting of the catalyst with cocatalyst and electron donor, and intensive mixing of the powder bed are

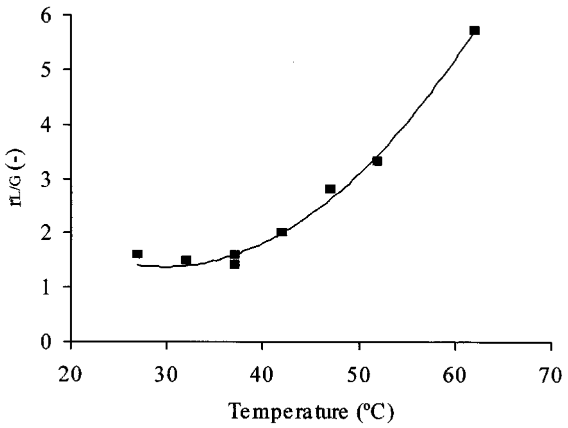

Figure 18. Ratio $r_{L/G}$ of the liquid- and gas-phase reaction rates as a function of the temperature.

crucial to obtain reproducible experiments with a highly active catalyst. Catalyst injection with a small amount of pentane into a reactor containing a support bed of NaCl crystals has been rather successful, although a few minutes are needed during the initial stage to evaporate the pentane from the reactor. Precontacting of the catalyst with PEEB at room temperature in the absence of TEAl keeps the catalyst inactive for a few minutes, during which the pentane is evaporated. Precontacting also decreases the catalyst activity by about 25%. Above pressures of 5 bar the reaction rate is proportional to the pressure; at pressures below 5 bar, the rates are significantly lower.

The kinetics were described by the same kinetic model as was used for liquid-phase reactions. The model describes the experiments moderately well for temperatures up to about 50°C; above 50°C the model is no longer valid due to a drastic increase in the deactivation rate.

Comparison of the reaction-rate curves obtained with the same catalyst as was used for the gas- and liquid-phase experiments show that the shape of the rate curves is the same, while the activity in the gas phase is lower. Below about 40°C, the reaction rates in the gas phase are about 35% lower than in the liquid phase; above 40°C, the rates in the gas phase are up to six times lower than in the liquid phase. During the first 5 to 15 min of gas-phase reactions the catalyst rapidly deactivates, which is attributed to thermal deactivation as a result of particle runaway.

Prepolymerization for a few minutes in pentane at ambient temperature increased the reaction rates and yields of the gas-phase polymerizations by about 15%. This increase is too small to explain the difference between the reaction rates in the gas and liquid phases.

In our future work, gas-phase polymerizations will be performed in larger reactors of steel and at higher pressures. Also, the influence of the prepolymerization variables will be studied in detail, and the kinetic data will be used to evaluate fluid-bed reactors for olefin polymerizations.

Acknowledgments

These investigations were supported by the Netherlands Foundation for Chemical Research (SON) with financial aid from NWO and STW. The technical assistance of K. van Bree, G. H. Banis, and A. Pleiter is gratefully acknowledged. G. van der Ven and J. Stokman are gratefully acknowledged for their contribution in the experimental work.

Notation

C^* = number of active sites, mol/g cat
K_D = overall deactivation constant, g cat/m^{-3}
t = time, h
T = temperature, K
R = gas constant, J/mol·K
x_m = mass fraction of monomer in the polymer

Subscripts

b = bulk
c = catalyst
exp = experiment
cat = catalyst
p = particle
r = reactor

Literature Cited

Doi, Y., T. Keii, E. Suzuki, and M. Tamura, "Propene Polymerization with a Magnesium Chloride Supported Ziegler Catalyst: 1," *Macromol. Chem.*, **183**, 2285 (1982).

Hutchinson, R. A., and W. H. Ray, "Polymerization of Olefines Through Heterogeneous Catalysis: VIII. Monomer Sorption Effects," *J. Appl. Poly. Sci.*, **41**, 51 (1990).

Samson, J. J. C., G. Weickert, A. E. Heerze, and K. R. Westerterp, "Liquid Phase Polymerization of Propylene with a Highly Active Catalyst," *AIChE J.*, **44**, 1424 (1998).

Samson, J. J. C., P. J. Bosman, G. Weickert, and K. R. Westerterp, "Liquid Phase Polymerization of Propylene with a Highly Active $MgCl_2/TiCl_4$/EB Catalyst: The Influence of Hydrogen, Cocatalyst and Electron Donor on Reaction Kinetics," *J. Poly. Sci.: Part A: Poly. Chem.*, **37**, 219 (1999).

Manuscript received Mar. 11, 1998, and revision received Mar. 18, 1999.